Effect of grain size distribution on plastic strain recovery

Marisol Koslowski*
School of Mechanical Engineering, Purdue University, West Lafayette, Indiana 47906, USA
(Received 12 July 2010; revised manuscript received 3 August 2010; published 17 August 2010)

Plastic deformation is size dependent, this is observed in experiments and simulations and has a fundamental effect in crystalline materials with average grain size in the nanometer range. Recent experiments show that plastic deformation is not only affected by the average grain size but also by the grain size distribution. One of the most notorious aspects is that nanocrystalline metals recover plastic strain after unloading. Here, we perform numerical simulations that show that plastic strain recovery is driven by the inhomogeneous stress distribution observed in samples with large variations in grain size. Our model predicts that the fraction of plastic strain recovery increases with the macroscopic strain applied to the sample and that the recovery rate increases as the volume fraction of larger grains decreases.

DOI: 10.1103/PhysRevB.82.054110 PACS number(s): 62.20.fq, 61.72.Ff, 62.20.Hg

I. INTRODUCTION

The mechanical response of polycrystalline metals is largely affected by their microstructure. It is observed that the yield stress of a polycrystalline metal increases as the grain size decreases following a power law. This is known as Hall-Petch effect.[1–5]

On the other hand, the effect of the grain size distribution in the mechanical response has not been well established. Recent experiments in nanocrystalline thin films[6–8] show that plastic strain is recovered under macroscopically stress-free conditions. The authors suggest that a broad grain size distribution produces a highly heterogeneous stress distribution and this is responsible for plastic strain recovery.

Rajagopalan *et al.*[6,7] conducted experiments in nanocrystalline aluminum and gold thin films with an average grain size of 65 nm and 50 nm, respectively. Both materials recover 50–100 % of plastic strain after unloading. Another feature observed in these experiments is that once the strain is recovered the specimen shows no residual hardening during the next loading. X-ray and deformation studies on crystalline aluminum with a bimodal distribution of grains (with grains in the range 40–400 nm) also suggest that plastic strain recovery requires the presence of sufficiently small and big grains to generate inhomogeneous stress distribution in the sample.[8] These findings reveal that the average grain size itself is not enough for a complete characterization of the microstructure in nanocrystalline materials but the grain size distribution should also be considered.

In this paper I present dislocation simulations of plastic deformation of polycrystalline materials with bimodal distribution of grains. The evolution of the dislocations is simulated with a phase field dislocation model.[9–11] The simulations show that large grains deform plastically while in the smaller grains the onset of plastic deformation occurs at larger applied stresses causing a inhomogeneous distribution of stress in the sample after plastic deformation.

After removal of the applied stress the stress in the small grains remains with the same sign that the applied stress while the stress in big grains changes sign. Therefore, at macroscopically zero stress, dislocations are under the influence of local stresses and by a thermally activated creep they relax the energy of the system resulting in macroscopic strain recovery. This effect is observed in our simulations only in the presence of a large grain size distribution in agreement with experiments.[6–8]

Our model also predicts that the rate of plastic strain recovery increases as the volume fraction of larger grains decreases and that the fraction of plastic strain recovered increases with the macroscopic applied strain. The later prediction is in agreement with experimental observation.[8] Experimental data to validate the former prediction is still not available.

II. PHASE FIELD DISLOCATION MODEL

The evolution of the dislocations in the grains are simulated with a phase field dislocation (PFD) model.[9–11] In this model an integer valued phase field describes the evolution of the dislocations. The value of the phase field, $\xi(\boldsymbol{x})$, accounts for the number of dislocations that have crossed over a point in the slip system. Grain boundaries are represented as barriers to the motion of dislocations and also act as dislocation sources. The elastic energy of the dislocation ensemble can be written as[9]

$$E[\xi(\boldsymbol{x})] = \int K(\boldsymbol{k})|\hat{\xi}(\boldsymbol{k})|^2 \frac{d^2k}{(2\pi)^2} - b\int \tau\xi(\boldsymbol{x})d^2x, \qquad (1)$$

where for simplicity, we consider a single slip plane. In Eq. (1) the first term in the right-hand side is the principal value of the integral, a superimposed $\hat{(\ )}$ denotes a Fourier transform, k_i are the components in the transformed Fourier space, τ is the resolved applied shear stress, b is the Burger's vector, and $K(\boldsymbol{k})$ is a nonlocal kernel that represents the elastic interaction between the dislocations that in two dimensions reduces to

$$K(\boldsymbol{k}) = \frac{\mu b^2}{4}\left(\frac{k_2^2}{\sqrt{k_1^2+k_2^2}} + \frac{1}{1-\nu}\frac{k_1^2}{\sqrt{k_1^2+k_2^2}}\right), \qquad (2)$$

where ν is the Poisson's ratio and μ is the shear modulus. The second term in Eq. (1) represents the interaction of the dislocations with the external applied stress. Kernels similar

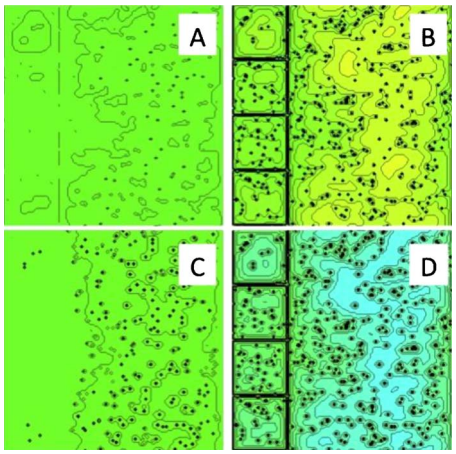

FIG. 1. (Color online) Dislocation pattern at stresses (a) $\tau=0.2\times10^{-2}\mu$, (b) $\tau=0.4\times10^{-2}\mu$, (c) $\tau=0$, and (d) $\tau=-0.4\times10^{-2}\mu$.

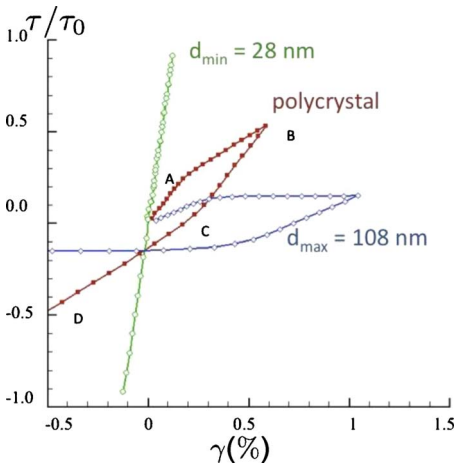

FIG. 2. (Color online) Stress-strain curve for the macroscopic polycrystal (filled squares) and local stress strain curves for the individual grains (open symbols), $\tau_0=10^{-2}\mu$.

to the one in Eq. (2) appear in nonequilibrium critical phenomenon involving an external force and a pinning potential.[10,12–14]

The pinning potential in the current model represents a random distribution of obstacles that describes forest dislocations. The irreversible obstacle interaction is built into the variational formulation by time discretization. We consider a sequence of discrete times and compute the phase field distribution ξ^{n+1} at time t_{n+1}, given the solution ξ^n at time t_n. The updated slip distribution follows from the minimization of the incremental work function

$$W[\xi^{n+1}|\xi^n] = E[\xi^{n+1}] - E[\xi^n] + \int f(\boldsymbol{x})|\xi^{n+1}(\boldsymbol{x}) - \xi^n(\boldsymbol{x})|d^2x. \tag{3}$$

The last term in Eq. (3) is the energy cost per unit area associated with the passage of one dislocation and $f(\boldsymbol{x})$ represents the obstacle distribution in the domain.

Grain boundaries are represented as impenetrable surfaces to dislocations impeding their motion. The confinement of dislocations to small grain domains predicts, in the current model, the size dependency of the yield stress. The PFD model has been applied successfully in the past to predict grain size dependency of the yield stress.[11,15]

III. EFFECTS OF GRAIN SIZE DISTRIBUTION

We carry out FPD simulations where we consider polycrystals with distributions of two grain sizes. All the configurations are characterized by the size of the small and large grains and the volume fraction of the big grains, f. Figure 1 shows one of such configurations with $f=0.67$. In all the configurations the smallest grain size lies between 10 and 57 nm while the largest grain is in the range 57–108 nm and we consider $f=0.5$, $f=0.67$, and $f=0.75$. The domain is 115 nm by 115 nm with periodic boundary conditions. We set the material constants to Aluminum with $E=70$ GPa, $\mu=26$ GPa, $\nu=0.35$, and $b=0.288$ nm.

Figure 1 shows the dislocation pattern in a domain with grain sizes $d_{min}=28$ nm and $d_{max}=108$ nm, and $f=0.67$ during a loading cycle. The model accounts for dislocation-dislocation interaction and therefore, naturally accounts for size effects in the yield stress.[11,15] The onset of plastic deformation occurs at higher stresses as the grain size becomes smaller.

The curve with the filled symbols in Fig. 2 shows the stress-strain behavior for the system in Fig. 1. The letters in the curve indicate the macroscopic stress corresponding to the dislocation patterns in Fig. 1. The other curves in the figure show the local stress-strain response of the small grains, $d_{min}=28$ nm and the big grains $d_{max}=108$ nm. The dislocation patterns in Figs. 1(B) and 1(D) clearly show a dark region with high dislocation density close to the grain boundaries. The pattern (C) corresponds to zero applied external stress and shows that dislocations in the small grains disappear when the applied stress is removed in the first cycle. This is in agreement with previous work of Budrovic *et al.*[16] where *in situ* x-ray measurements were carried out during plastic deformation in nanocrystalline Nickel with 26 nm mean grain size. These experiments show that there is no build up of residual dislocations upon unloading. The same experiments show that this effect is not observed in polycrystalline Cu with average grain size 20 μm.

At point A in Fig. 2 the macroscopic stress curve shows the onset of plastic response, even though only the big grains deform plastically, while the small grains remain elastic. This effect is only observed when the ratio between the grain sizes is such that the yield stress in the smaller grains is much higher than in the big grains due to Hall-Petch effect. This difference in the yield stress causes an inhomogeneous stress distribution in nanocrystalline samples and were reported in Al membranes deformed plastically.[17] This inhomogeneous stress distribution is proposed to be the cause of observed reverse stress relaxation in plastically deformed thin films.[18]

Figure 3 shows the stress on two grains as a function of the macroscopic strain during loading and unloading up to zero macroscopic stress. In this simulation the grains have size $d_{min}=28$ nm and $d_{max}=80$ nm and a volume fraction $f=0.5$, here the small grains also deform plastically. The dashed lines correspond to a loading condition with maxi-

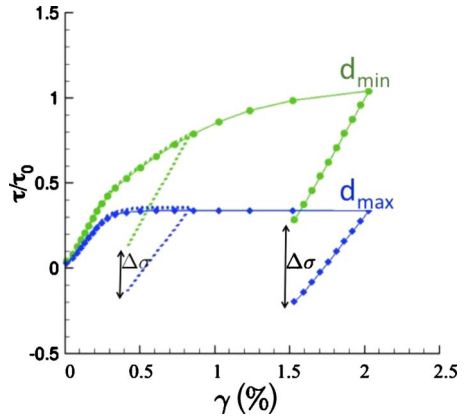

FIG. 3. (Color online) Local stress versus macroscopic strain for two grains of size d_{min}=28 nm and d_{max}=80 nm, and f=0.5

mum average strain γ_{max}=0.8% and the solid line corresponds to a maximum strain γ_{max}=2%. This figure can be used to define the yield stress on each individual grain by the 0.2% offset, i.e., the yield stress for each grain is the local stress at this grain at which the average deformation reaches 0.2%.

Figure 4 shows stress-strain curves for two grains in another configuration with d_{min}=56 nm and d_{max}=80 nm, and f=0.5. The size of the large grain is the same that the one showed in Fig. 3 and therefore, the yield stress in the large grain attains the same value. On the other hand, the yield stress of the small grain decreases as the grain size increases as expected.[1,2]

In both cases the resolved shear stress in the small grains remains in the same direction that the applied shear stress upon removal of the macroscopic load while in the large grains the stress changes sign. The simulations show that the difference in stress between the small and large grains upon removal of the macroscopic stress, $\Delta\sigma$, augments with the maximum macroscopic strain. This inhomogeneous stress distribution is caused by the variations in grain size that lead to soft large grains and harder small grains. The same behavior is observed for the whole range of grain sizes in our simulations. In the following section we show that this inhomogeneous stress distribution shown in Figs. 3 and 4 is the

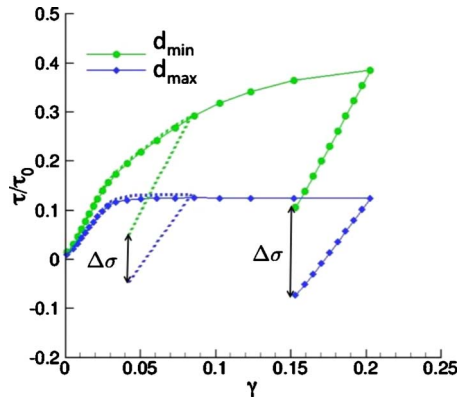

FIG. 4. (Color online) Local stress versus macroscopic strain for two grains of size d_{min}=56 nm and d_{max}=80 nm, and f=0.5.

cause of plastic strain recovery with a simplified creep model.

IV. PLASTIC STRAIN RECOVERY

During plastic deformation there is a large variation in the state of stress of the individual grains in the simulated domain. At zero macroscopic stress the stress in large grains remains with the same sign that the applied stress while the stress in the small grains changes sign causing a state of inhomogeneous residual stress in the sample. After removal of the applied stress the large grains relax their residual stress by creep deformation. As a result, a macroscopic strain recovery is observed in the polycrystalline sample.

Plastic strain recovery is a thermally activated process, in the following we will use a classical creep model to model the evolution of the strain with time of the form:[19,20]

$$\dot{\gamma}(t) = \dot{\gamma}_0 \left(\frac{\tau}{\mu}\right)^n, \tag{4}$$

where τ is the resolved shear stress, $\dot{\gamma}_0$ is a scale factor of the strain rate, and n gives the stress dependency of the strain rate. When creep is controlled by dislocation glide $n \sim 4$.[20] The strain rate factor, $\dot{\gamma}_0$, incorporates the strain rate controlling mechanisms as well as thermal activation as follows:

$$\dot{\gamma}_0 = \dot{\gamma}_{sr} e^{-E_a/kT}, \tag{5}$$

where k is the Boltzman's constant, T is the absolute temperature, E_a is an activation energy, and $\dot{\gamma}_{sr}$ depends only on the strain rate.[19,20]

Assuming a parallel arrangement of small and large grains we can obtain a closed form solution for the evolution of the plastic strain in Eq. (4). Under this assumption the strain is equal in the small and large grains and the average resolved shear stress in the large grains, τ^b, and the average resolved shear stress in the small grains, τ^s satisfy the following relation:

$$f\tau^b + (1-f)\tau^s = \tau_m, \tag{6}$$

where τ_m is the macroscopic stress of the sample. The response of the crystalline system is more complicated but this simplification will allow us to study the effect of grain volume fraction, maximum deformation, and grain size. We also assume that small grains deform elastically in the whole range of deformation while large grains deform elastically up to a yield stress, τ_y. After that, they follow a perfect plastic deformation law. The stress in the small grains follows a linear elastic relation $\tau^s = \mu\gamma$. Therefore Eq. (6) at zero macroscopic stress results

$$f\tau_0^b + (1-f)\mu\gamma_r = 0, \tag{7}$$

where γ_r is the macroscopic deformation at zero macroscopic stress and τ_0^b is the stress in the large grains at zero macroscopic stress. This simplified model shows the same overall behavior that the simulations shown in the previous section. In particular, as the macroscopic strain increases the difference between the stress in the large and small grains also increases as shown in Figs. 3 and 4.

We will assume that the macroscopic creep deformation is driven by the relaxation of the large grains that undergo plastic deformation. Therefore, the average plastic strain, γ_r evolves controlled by the stress in the large grains as

$$\dot{\gamma}_r(t) = \dot{\gamma}_0 \left(\frac{\tau_0^b}{\mu} \right)^n . \tag{8}$$

Even though this is a simplified model with only two grain sizes, Eq. (8) reveals that plastic strain recovery by creep operates only in the presence of inhomogeneous stress distributions. Also, as the maximum plastic strain increases, our simulations show that τ_0^b becomes larger in magnitude increasing the rate of recovery in agreement with experiments.[16]

As strain recovery evolves the stress, τ_0^b decreases in magnitude following Eq. (7). Replacing Eq. (7) in Eq. (8) we obtain the following differential equation for γ_r:

$$\dot{\gamma}_r(t) = \dot{\gamma}_0 \left(\frac{1-f}{f} \right)^n \gamma_r^n . \tag{9}$$

It is clear from this equation that the volume fraction affects the rate of strain recovery. For a material with a unique grain size, $f=1$, the strain recovery rate is zero in agreement with experiments that show no plastic strain recovery in thin films with unimodal grain distributions.[7] As the volume fraction of large grains decreases the stress τ_0^b in the large grains increases in magnitude accelerating the rate of strain recovery. The evolution of the strain follows from the integration of Eq. (9) as

$$\gamma_r(t) = \left[\gamma_r(0) - (n-1)\dot{\gamma}_0 \left(\frac{1-f}{f} \right)^n t \right]^{1/(n-1)}, \tag{10}$$

where $\gamma_r(0) = f(\gamma_{max} - \tau_y/\mu)$ is the initial macroscopic deformation.[21,22] Figure 5 shows the evolution of the strain at zero macroscopic stress given by Eq. (10) yield stress in the large grains of $\tau_y = 180$ MPa, $n=4$, and $\dot{\gamma}_0 = 1 \times 10^7$ s^{-1}.

In Rajagopalan's[7] experiments in Al free standing thin films the maximum strain is $\gamma_{max} = 1.4\%$ and the grain volume fraction $f=0.8$. The solid curve in Fig. 5 shows the solution of Eq. (10) for these deformation conditions, the plastic strain recovers by 50% in 1000 s in very good agreement with the experimental values.

The model predicts a larger fraction of recovery for larger maximum applied deformation in agreement with experimental observation.[16] Figure 5 also shows the effect of changes in volume fraction, f. As the volume fraction of large grains decreases the plastic strain recovery rate increases. Our results show that for $\gamma_{max} = 1.4\%$ and $f=0.6$ the plastic strain recovers by 80% and with $f=0.4$ the plastic strain recovers by 87% in 1000 s.

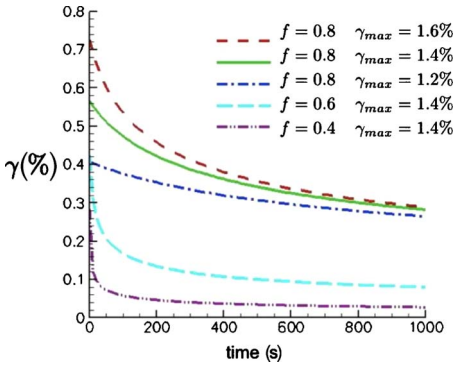

FIG. 5. (Color online) Plastic strain recovery dependency on the volume fraction and maximum deformation.

V. SUMMARY AND CONCLUSIONS

The present results show that plastic strain recovery is driven by the inhomogeneous stress distribution in plastically deformed nanocrystalline materials. Our model shows that increasing the applied plastic deformation augments the plastic strain recovery in very good agreement with experimental results.[16] On the other hand, for a fixed maximum deformation γ_{max} the recovery rate increases as the fraction of large grains decreases.

That plastic strain recovery is caused by a grain size distribution has important implications for the interpretation of deformation mechanisms in nanocrystalline materials. It was suggested that plastic strain recovery is driven by grain boundary accommodation.[23] Our simulations do not include this mechanism but yet predicts the correct behavior. This implies that plastic strain recovery may be driven by a combination of both mechanisms but at room temperature and with grains in the 10–100nm range the plastic deformation of big grains surrounded by elastically deforming small grains are the dominant mechanisms as suggested also by atomistic simulations.[24] Most important, the present results reveal that average grain size itself is not enough for a complete characterization of the microstructure in nanocrystalline materials but variations in the grain size distribution should also be considered.

ACKNOWLEDGMENTS

This work was performed under the auspices of the United States Department of Energy office of Basic Energy Sciences under Contract No. DE-FG02-07ER46398 and the Department of Energy, National Nuclear Security Administration under Award No. DE-FC52-08NA28617.

*marisol@purdue.edu

[1] E. O. Hall, Proc. Phys. Soc., London, Sect. B **64**, 747 (1951).
[2] N. J. Petch, J. Iron Steel Inst., London **174**, 25 (1953).
[3] M. D. Uchic, D. M. Dimiduk, J. N. Florando, and W. D. Nix, Science **305**, 986 (2004).
[4] Y. Xiang, T. Y. Tsui, and J. Vlassak, J. Mater. Res. **21**, 1607 (2006).
[5] A. T. Jennings, M. J. Burek, and J. R. Greer, Phys. Rev. Lett. **104**, 135503 (2010).
[6] J. Rajagopalan, J. H. Han, and T. A. Saif, Science **315**, 1831 (2007).
[7] J. Rajagopalan, J. H. Han, and T. A. Saif, Scr. Metall. **59**, 921 (2008).
[8] I. Lonardelli, J. Almer, G. Ischia, C. Menapace, and A. Molinari, Scr. Mater. **60**, 520 (2009).
[9] M. Koslowski, A. Cuitiño, and M. Ortiz, J. Mech. Phys. Solids **50**, 2597 (2002).
[10] M. Koslowski, R. LeSar, and R. Thomson, Phys. Rev. Lett. **93**, 265503 (2004).
[11] M. Koslowski, Philos. Mag. **87**, 1175 (2007).
[12] S. Zapperi, A. Vespignani, and H. Stanley, Nature (London) **388**, 658 (1997).
[13] M. Kardar, Phys. Rep. **301**, 85 (1998).
[14] J. P. Sethna, K. Dahmen, and C. Myers, Nature (London) **410**, 242 (2001).
[15] A. Hunter and M. Koslowski, J. Mech. Phys. Solids **56**, 3181 (2008).
[16] Z. Budrovic, H. Van Swygenhoven, P. M. Derlet, S. Van Petegem, and B. Schmitt, Science **304**, 273 (2004).
[17] R. Spolenak *et al.*, Phys. Rev. Lett. **90**, 096102 (2003).
[18] R. Spolenak, C. A. Volkert, S. Ziegler, C. Panofen, and W. L. Brown, MRS Symposia Proceedings No. 673 (Materials Research Society, Pittsburgh, 2001), p. 141.
[19] A. Argon and A. K. Bhattacharya, Acta Metall. **35**, 1499 (1987).
[20] U. F. Kocks, A. S. Argon, and M. F. Ashby, in *Progress in Materials Science*, edited by B. Chalmers, J. W. Christian, and T. B. Massalski (Pergamon Press, Oxford, 1975), Vol. 19.
[21] M. Carmen Miguel, A. Vespignani, M. Zaiser, and S. Zapperi, Phys. Rev. Lett. **89**, 165501 (2002).
[22] T. Sullivan, M. Koslowski, F. Theil, and M. Ortiz, J. Mech. Phys. Solids **57**, 1058 (2009).
[23] Y. Wei, A. F. Bower, and H. Gao, Scr. Mater. **57**, 933 (2007).
[24] X. Li, Y. Wei, W. Yang, and H. Gao, Proc. Natl. Acad. Sci. U.S.A. **106**, 16108 (2009).